Nonlinear Parameter Estimation of Steady-State Induction Machine Models

Antonio Marcus Nogueira Lima, *Member, IEEE*, Cursino Brandão Jacobina, *Member, IEEE*, and Eurico Bezerra de Souza Filho

***Abstract*—The use of modern identification techniques in determining the values of the steady-state equivalent circuit parameters of a three-phase squirrel-cage induction machine is discussed. The identification procedure is based on the steady-state phase current versus slip and input power versus slip characteristics. The proposed identification algorithm is of a nonlinear kind. The machine parameters are obtained as the solution of a minimization of least-squares cost function of the difference between calculated and experimental steady-state characteristics. Simulation, as well as experimental results concerning the application of the proposed algorithm to the modeling of a 1.5-kW wound-rotor three-phase induction machine, are presented.**

***Index Terms*— Induction machines, nonlinear estimation, parameter estimation.**

I. Introduction

KNOWLEDGE of the electrical and mechanical machine parameters is, to some extent, the touchstone in the analysis and design of both dc and ac motor drive systems. In the case of an ac induction motor drive, the electrical parameters are, generally, determined via the classical locked-rotor and no-load tests.

Estimation of the performance behavior of an induction machine is normally done by plotting the steady-state slip curves. To generate the data for plotting, one must use the equivalent circuit relations and the experimental results obtained from the above-mentioned classical tests. The comparison of these curves with those obtained by direct experimentation reveals significant differences in the entire range of slip varying from 0 to 1. This leads to the conclusion that, to describe the performance of the induction machine more precisely, one must modify the parameters obtained from the classical tests, in order to reduce the differences between the estimated and real performances.

To achieve this goal, the use of system identification algorithms appears to be a very promising approach. These algorithms allow one to take into account the effect of measurement errors, disturbances, and random signals on the estimated parameters. Concerning the use of system identification techniques to characterize an induction machine, one may devise two basic approaches. In the first one, the modeling is based on steady-state equations and leads, in general, to the use of equivalent circuit relationships [1]–[5], whereas, in the other approach, the machine characterization is addressed using dynamic model equations [6]–[8].

Manuscript received January 5, 1995; revised September 15, 1996.

The authors are with the Departamento de Engenharia Elétrica, Universidade Federal da Paraíba, 58109-970 Campina Grande, Paraíba, Brazil.

Publisher Item Identifier S 0278-0046(97)04139-7.

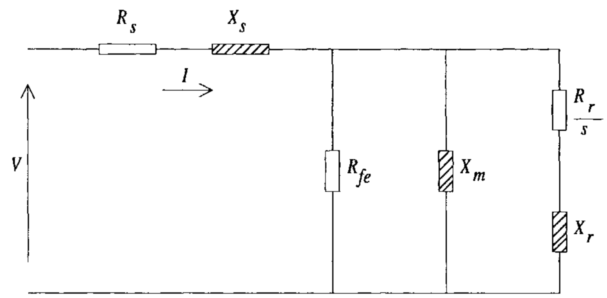

Fig. 1. Equivalent circuit of a squirrel-cage induction machine—single cage.

The equations relating the phase current to the slip and the circuit parameters involve many variables and are nonlinear. This fact does not enable one to directly use the many parameter estimation procedures existing in the literature. This fact implies increased complexity, since the nonlinear estimation problems are normally solved using *ad hoc* procedures.

In this paper, the estimation of the parameters of the equivalent circuit of a squirrel-cage induction machine is formulated as a nonlinear least-squares minimization problem. We start by defining a parametric vector containing the values of the stator and rotor resistances and the stator, rotor, and mutual inductances. The initial values for the components of this vector are obtained from the classical tests [9]. During the execution of the estimation algorithm, we use the steady-state characteristic curves of both the input power and the stator current to adjust the initial parameter vector. The data supplied to the estimation algorithm is basically collected as specified by the speed-current curve procedure [9]. The difference between the proposed experimental test and the procedure specified in the IEEE Standards is that the data concerning the active power absorbed by the motor, as well as the power factor, are recorded together with the current measurements. Then, there is no special requirements to conduct the proposed experimental tests.

II. Machine Model

The steady-state operation of a squirrel-cage induction machine supplied with a three-phase symmetrical voltage source can be described using the equivalent circuit shown in Fig. 1. The typical assumptions used when developing this model are borrowed from Chatelain [10]. The variables are referred to the stator reference frame.

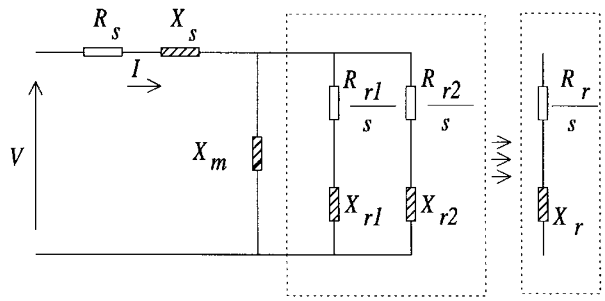

Fig. 2. Equivalent circuit of a squirrel-cage induction machine—double cage.

The equations of the stator current $I(s)$, the input power $P(s)$, and the electromagnetic torque $T(s)$ for a single-cage induction machine, deduced from the circuit of Fig. 1, are expressed as follows:

$$I(s) = V\sqrt{\frac{C^2+D^2}{A^2+B^2}} \tag{1}$$

$$P(s) = 3V^2\frac{AC-BD}{A^2+B^2} \tag{2}$$

$$T(s) = 3V^2\frac{p}{w}\frac{R_{fe}^2 R_r/s}{A^2+B^2}. \tag{3}$$

where V is the line voltage, w is the stator angular frequency, and s is the machine slip. The terms A, B, C, and D are obtained from the following expressions:

$$A = X_s\left(\frac{R_{fe}R_r}{sX_m} - X_r\right) + R_s\left(\frac{R_r}{s} + R_{fe}\left(1+\frac{X_r}{X_m}\right)\right) + \frac{R_{fe}R_r}{s} \tag{4}$$

$$B = X_s\left(\frac{R_r}{s} + R_{fe}\left(1+\frac{X_r}{X_m}\right)\right) - R_s\left(\frac{R_{fe}R_r}{sX_m} - X_r\right) + R_{fe}X_r \tag{5}$$

$$C = \frac{R_r}{s} + R_{fe}\left(1+\frac{X_r}{X_m}\right) \tag{6}$$

$$D = \frac{R_{fe}R_r}{sX_m} - X_r. \tag{7}$$

In the above equations, R_s, R_r, and R_{fe} are the stator, rotor, and iron losses equivalent resistances, respectively. Also, X_s, X_r, and X_m are the stator leakage, rotor leakage, and magnetizing reactances, respectively.

Equations (1)–(3) may be used to plot the steady-state characteristic slip curves by varying the slip from the locked-rotor condition ($s = 1$) to the no-load one ($s = 0$).

For a double-cage machine, neglecting the iron losses, one must add a second branch in parallel with the magnetizing reactance, as shown in Fig. 2.

The equations of the stator current $I(s)$ and the input power $P(s)$ are still given by (1) and (2), respectively, while, the electromagnetic torque $T(s)$ is expressed by

$$T(s) = 3V^2\frac{p}{w}\frac{R_r/s}{A^2+B^2}. \tag{8}$$

In (1), (2), and (8), the terms A, B, C, D, R_r, and X_r are obtained from the following expressions:

$$A = R_s\left(1+\frac{X_r}{X_m}\right) + \left(1+\frac{X_s}{X_m}\right)\frac{R_r}{s} \tag{9}$$

$$B = X_r + X_s\left(1+\frac{X_r}{X_m}\right) - R_s\left(\frac{R_r/s}{X_m}\right) \tag{10}$$

$$C = 1 + \frac{X_r}{X_m} \tag{11}$$

$$D = \frac{R_r/s}{X_m} \tag{12}$$

$$R_r = \frac{R_{r1}R_{r2}(R_{r1}+R_{r2}) + (R_{r1}X_{r2}^2 + R_{r2}X_{r1}^2)s^2}{(R_{r1}+R_{r2})^2 + (X_{r1}+X_{r2})^2 s^2} \tag{13}$$

$$X_r = \frac{X_{r1}X_{r2}(X_{r1}+X_{r2})s^2 + R_{r1}^2X_{r2} + R_{r2}^2X_{r1}}{(R_{r1}+R_{r2})^2 + (X_{r1}+X_{r2})^2 s^2}. \tag{14}$$

As can be noted, (1)–(3) and (1), (2), and (8) involve nonlinear functions to describe the steady-state slip curves.

III. Nonlinear Estimation

In order to determine the equivalent circuit model parameters from the slip curves, one must deal with a nonlinear curve-fitting problem. This problem is stated as the solution of the following minimization problem:

$$\min_{\theta\in\Omega} J(\theta) = \frac{1}{N}\sum_{i=1}^{N}[y_i - Y(s_i,\theta)]^2 \tag{15}$$

where

- $J(\theta)$ least squares cost function, i.e., the sum of the squares of the differences between the experimental and calculated slip curves;
- Ω parameter space of dimension l—the particular value of l depends on the number of parameters to be estimated;
- y_i ith experimental data value collected from a machine test $(I(s_i), P(s_i)$ or $T(s_i))$;
- $Y(s_i,\theta)$ nonlinear function relating the measured data $(I(s_i), P(s_i)$ or $T(s_i))$, the circuit parameters and the slip (s_i);
- θ parameter vector pertaining to Ω;

$$\theta = [\theta(1) \quad \theta(2) \quad \cdots \quad \theta(l-1) \quad \theta(l)]^T \tag{16}$$

single cage:

$$\theta = [R_r \quad X_r \quad X_s \quad R_s \quad X_m \quad R_{fe}]^T, \qquad l = 6 \tag{17}$$

single cage:

$$\theta = [R_r \quad X_r \quad X_s \quad X_m]^T, \qquad l = 4 \tag{18}$$

double cage:

$$\theta = [R_{r1} \quad R_{r2} \quad X_{r1} \quad X_{r2} \quad X_s]^T, \qquad l = 5 \tag{19}$$

double cage:

$$\theta = [R_{r1} \quad R_{r2} \quad X_{r1} \quad X_{r2} \quad X_s \quad R_s \quad X_m]^T, \qquad l = 7 \tag{20}$$

where s_i is the ith machine slip value and N is the length of experimental data vector.

The specific equation for $Y(s_i, \theta)$ depends on the kind of available experimental data. In all the cases, to obtain a parameter vector θ that minimizes the quadratic performance index defined by (15), one must deal with a nonlinear algorithm. This kind of problem is a quite general one, and some numerical problems may arise. A direct approach would require writing down the l (the length of θ) normal equations and developing an iterative technique for solving them [11]. The methods for numerical minimization of $J(\theta)$ consist of updating the estimated parameter vector θ_i according to

$$\theta_i = \theta_{i-1} + \mu_{i-1} R_{i-1}^{-1} \nabla J(\theta_{i-1}) \tag{21}$$

where $\nabla J(\theta)$ is the gradient of $J(\theta)$ and R_{i-1}^{-1} is a search direction matrix calculated using the information about $J(\theta)$ up to i^{th-1} instant. μ_{i-1} is a positive scalar chosen to insure an appropriate decrease of $J(\theta)$ [12].

In the computation of the inverse of the matrix R_{i-1}, some numerical problems may arise, and this actually depends on the kind of nonlinear function involved. The matrix inversion in (21) can be avoided using the steepest descent technique [12], but this leads to a very slow convergence algorithm. However, in order to obtain fast convergence algorithms, one must necessarily deal with the matrix inversion problem.

In the present identification problem, the kind of nonlinear functions involved (1)–(3) and (1), (2), and (8) leads to an ill-conditioned R_{i-1}. A very clumsy technique was reported in [4] to proceed with the matrix inversion in (21). In order to obtain consistent results, they developed special multidimensional algorithms that require the measurement of the stator current, the input power, and the electromagnetic torque. Besides the numerical complexity of these algorithms, it is important to note that their major drawback is the need for the measurement of the electromagnetic torque. The torque measurement requires the use of special instrumentation, since it involves the use of mechanical moving parts.

In this paper, a recursive algorithm is proposed to solve the minimization problem stated in (15). The proposed approach avoids the above-mentioned numerical problems and yields good results requiring the measurement of electrical quantities only. The recursive algorithm is developed using the matrix inversion lemma [13].

In the proposed estimation technique, the adjustment of the parameter vector is obtained using the following relations:

$$\theta_i = \theta_{i-1} + W_i G_i [y_i - Y(s_i, \theta_0)] \tag{22}$$

$$W_i = W_{i-1} - \frac{W_{i-1} G_i G_i^T W_{i-1}}{1 + G_i^T W_{i-1} G_i} \tag{23}$$

where

$$G_i = \left[\frac{\partial Y(s,\theta)}{\partial \theta(1)} \quad \frac{\partial Y(s,\theta)}{\partial \theta(2)} \quad \cdots \quad \frac{\partial Y(s,\theta)}{\partial \theta(l)} \right]^T_{\theta=\theta_0, s=s_i} \tag{24}$$

and

θ_0 initial parameter vector;
W_i weighting matrix;
s_i ith slip value.

Starting from the initial parameter vector θ_0, and using the measured data of y_i and s_i, we adjust the actual θ_i in order to reduce the square of the difference between $Y(s_i, \theta_0)$, and y_i. $Y(s_i, \theta_0)$ is a prediction of y_i obtained using the parameter vector θ_0.

The basic structure of the estimation algorithm is best explained by going through the ten steps shown below.

1) Obtain the y_i data.
2) Set up the initial values of the parameter vector θ_i (θ_0) and weighting matrix W_i (e.g., $W_0 = 10^3 I_l, I_l$ being an l dimension square identity matrix).
3) Compute the derivative (numerical/analytical) of the nonlinear function $Y(s_i, \theta_0)$.
4) Compute the prediction residuals $[y_i - Y(s_i, \theta_0)]$.
5) Cumulate the terms of $J(\theta)$.
6) Update the parameter vector θ_i and the weighting matrix W_i.
7) Repeat steps 3)–6) to use up all the data from the slip curves.
8) Check θ_N and stop the procedure if any of its component does not have a physical meaning $(\theta_N(j) < 0, j = 1, l)$.
9) Check $J(\theta)$ and successfully stop the procedure if its value is lower than a prescribed threshold limit (e.g., 10^{-4}).
10) Iterate the procedure from step 3). If $J(\theta_N) > J(\theta_0)$ then $\theta_0 = \theta_0$ and $W_0 = W_0/2$, otherwise, $\theta_0 = \theta_N$ and $W_0 = W_N$.

The partial derivatives needed to implement the algorithm may be calculated using either numerical differentiation techniques or its analytical expression (see the Appendix). In both cases, for the present models, the algorithm works without problems.

The choice of the initial parameter θ_0 is somewhat crucial. In general, the initial parameter θ_0 cannot be set to zero and must be "close" to the "true" θ. This problem is quite common in this kind of least-squares problem, as reported in [11]. However, in the present case, the choice of θ_0 may be anchored in the previous knowledge of the user about the machine to be characterized. That is, the user knows, or has determined by the classical tests, the so-called standard machine parameters and may set θ_0 equal to them.

IV. Simulation Results

To evaluate the performance of the above algorithm, a digital simulation program was developed. As the first step, the proposed algorithm was formulated and employed to estimate the circuit parameters of a double-cage induction machine, the characterization of which had been done in [4]. The equivalent circuit model employed is shown in Fig. 2.

Equations (1) and (4)–(7) establish the relationship between the stator current, the slip, and the parameters. This equation set was used to simulate the "experimental" data (y_i). A pseudorandom Gaussian number generator was used to simulate the measurement noise. In the simulation case study, the number of "experimental" data points was fixed to 50 $(N = 50)$. When using the power slip curve we must use (2) and (4)–(7).

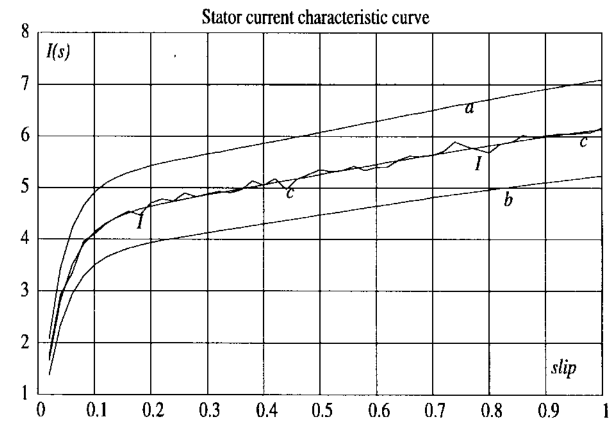

Fig. 3. Convergence of the recursive algorithm.

Fig. 3 illustrates the convergence of the proposed algorithm. The curves marked with a and b were plotted using the two parameter vectors used to start up the simulation program. The final values are obtained after ten iterations. The initial and final parameter vectors are

$$\theta_{0a} = [0.083\ \ 0.016\ \ 0.01\ \ 0.14\ \ 0.144\ \ 0.0078\ \ 4.3]^T$$
$$\theta_{0b} = [0.07\ \ 0.01\ \ 0.009\ \ 0.1\ \ 0.1\ \ 0.0078\ \ 4.3]^T$$
$$\theta_{Na} = [0.064\ \ 0.011\ \ 0.002\ \ 0.114\ \ 0.094\ \ 0.064\ \ 4.3]^T$$
$$\theta_{Nb} = [0.063\ \ 0.011\ \ 0.0017\ \ 0.114\ \ 0.094\ \ 0.064\ \ 4.3]^T.$$

The curve c was generated with the "true" parameter vector. Also, the curves obtained using θ_{Na} and θ_{Nb} are plotted in this same figure, but there is no visible difference between them and curve c. The "true" parameter vector is

$$\theta = [0.0693\ \ 0.0132\ \ 0.00843\ \ 0.1162\ \ 0.123\ \ 0.00778\ \ 4.3]^T.$$

The curve I ($=$ curve $c +$ noise) represents the measured current on which the noise measurement (noise covariance $= 1$) is included. The values from the curve I are the "experimental" data y_i used in the estimation algorithm.

As can be seen from Fig. 3, in both cases, the algorithm converges to the curve c, which corresponds to the "true" parameter vector. In this simulation study, as well as in the experimental one, the variables are expressed in the standard p.u. system.

The performance of the algorithm when only the data from the stator-current slip curve is used and θ_i includes all the equivalent circuit parameters $([R_{r1}\ \ R_{r2}\ \ X_{r1}\ \ X_{r2}\ \ X_s\ \ R_s\ \ X_m]^T, l = 7)$ is not satisfactory. Indeed, if one wishes to use the final parameter vector θ_{Na} or θ_{Nb} to plot the power slip curve, the differences from the "real" one are significant. Fig. 4 shows the "real" input power slip curve (curve c) and the curves generated with the θ_{Na} (curve a) and θ_{Nb} (curve b).

However, supposing that R_s and X_m are known *a priori* and fixed over the entire slip range, better results may be obtained. In fact, using only the stator-current slip curve and a parametric vector of reduced dimension ($l = 5$), the above-mentioned differences become negligible. Otherwise, if it is desirable to include R_s and X_m in the parameter vector, it is necessary to consider an augmented measurement data vector to obtain consistent results.

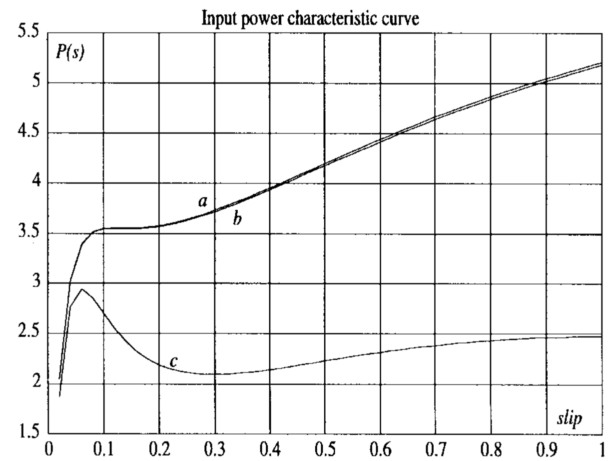

Fig. 4. Power slip curve obtained with a parameter vector of dimension 7 using only the stator current data.

The proposed algorithm was then modified to process an augmented measurement data vector, including both the stator current and input power data. To use the data from the stator-current and input-power slip curves, it is necessary to restate the above-mentioned minimization problem, redefining the least square cost function $J(\theta)$ as

$$J_{ip}(\theta) = \frac{1}{N}\sum_{i=1}^{N}[I(s_i) - I(s_i,\theta)]^2 + \frac{1}{N}\sum_{i=1}^{N}[P(s_i) - P(s_i,\theta)]^2. \tag{25}$$

In (25), $I(s_i)$ and $P(s_i)$ are the experimental data of the stator current and input power, respectively. Also, $I(s_i,\theta)$ and $P(s_i,\theta)$ are the nonlinear functions derived from the equivalent circuit model.

Starting from (25), we obtain the modified recursive algorithm, which is slightly different from the one presented above. In the modified algorithm, it is necessary to process $2N$ data points (N for the current slip curve and N for the power slip curve). Allowed by this particular form of $J_{ip}(\theta)$, the algorithm computation is done as follows.

The estimation procedure begins with θ_{0I} and W_{0I}. The first N computations are done using only the stator-current data points. At the end of these computations, the parameter vector and the weighting matrix evolves to θ_{NI} and W_{NI}. Next, the processing of the power data points start using θ_{NI} and W_{NI} as initial values. When using the power data points, it is necessary to change the G_i vector as is indicated in (27). When final values θ_{NP} and W_{NP} are obtained, the checking steps 8) and 9) (see Section III) are executed. If the procedure has to be restarted, we set $\theta_{0I} = \theta_{NP}$ and $W_{0I} = W_{NP}$ and change derivative vector G_i. The derivative vector G_i for the

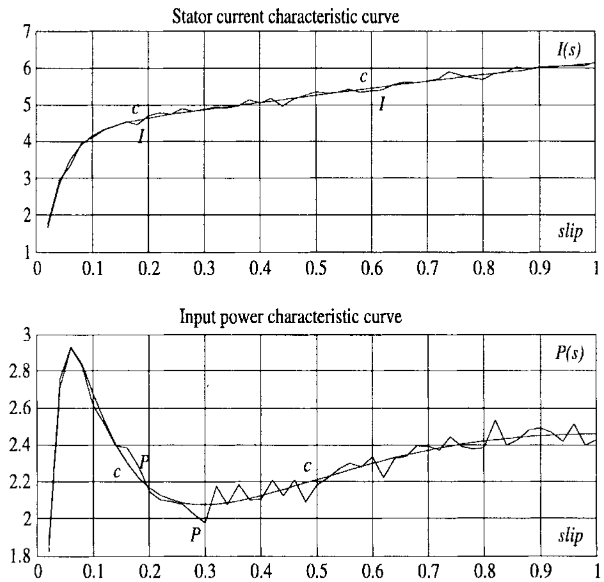

Fig. 5. Current and power slip curves obtained with a parameter vector of dimension 7, using both the stator and input power data.

modified recursive algorithm is given by

$$G_i = \left[\frac{\partial I(s,\theta)}{\partial\theta(1)} \cdots \frac{\partial I(s,\theta)}{\partial\theta(l)}\right]^T_{\theta=\theta_0, s=s_i} \quad 1 \le i \le N \tag{26}$$

$$G_i = \left[\frac{\partial P(s,\theta)}{\partial\theta(1)} \cdots \frac{\partial P(s,\theta)}{\partial\theta(l)}\right]^T_{\theta=\theta_0, s=s_i} \quad N+1 \le i \le 2N. \tag{27}$$

Changing the order of the current data and power data processing has no influence on the final results.

Fig. 5 shows the results obtained using the modified recursive algorithm. The upper half of this figure shows the "experimental" stator-current slip curve (curve I) and the one (curve c) plotted with the estimated parameters. In the lower part, in this figure, there is the "experimental" input-power slip curve (curve P) and its estimated version (curve c).

We note that the curves of current and power plotted with the estimated parameters agreed reasonably well with the "real" ones. The initial and final parameter vectors in this case are the following:

$$\theta_{0a} = [0.083 \;\; 0.016 \;\; 0.01 \;\; 0.14 \;\; 0.144 \;\; 0.0078 \;\; 4.3]^T$$
$$\theta_{Na} = [0.078 \;\; 0.0129 \;\; 0.0164 \;\; 0.121 \;\; 0.1167 \;\; 0.0073 \;\; 4.29]^T.$$

V. Experimental Results

The proposed estimation algorithm was employed to estimate the parameters of a three-phase wound-rotor induction machine. The experimental data (y_i) were collected from the laboratory tests. The length of the experimental data vector is 34 $(N = 34)$ and the estimation algorithm iterates 50 times to yield the parameters. It is important to remark that the proposed algorithm is intended to be executed off-line. In this case, the estimation algorithm, coded in Matlab script format, takes approximately 40 s (this time estimated with

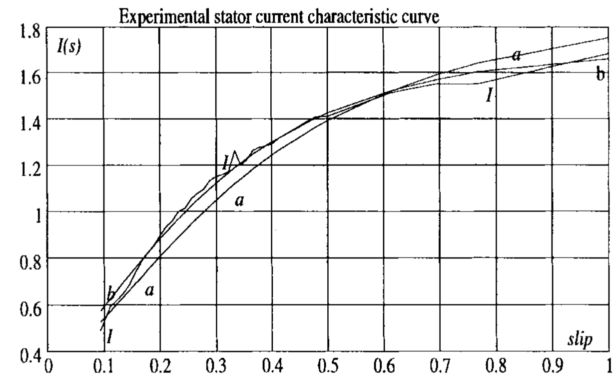

Fig. 6. Experimental and estimated stator-current slip curves.

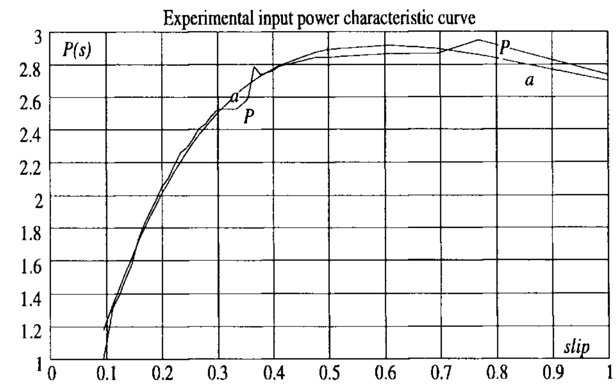

Fig. 7. Experimental and estimated input-power slip curves.

function `etime` of Matlab 4.2c1 for Windows running in a $486DX4$–100 MHz) to yield the estimates presented as follows. In fact, the proposed methodology must be considered as one step further after collecting the data from the standard tests (i.e., the recommended IEEE test procedures [9]). A wound-rotor machine was chosen, in order to enable the study of the effect of the rotor resistance on the performance of the algorithm. All the data available about that machine is the nameplate data given below.

Power: 1.5 kW—Voltage: 380/220 V—Current: 5.8/3.4 A
Frequency: 60 Hz—Poles: 4—$\cos\phi$: 0.86.

In the experimental case study, the recursive parameter estimation algorithm was developed using (1)–(3). Both the stator-current and the input-power data vector were employed in the estimation algorithm. The initial and the estimated parameter vectors are the following:

initial values—

$$\theta_0 = [3.068 \;\; 3.958 \;\; 3.958 \;\; 2.014 \;\; 43.99 \;\; 300]^T$$

estimated values—

$$\theta_N = [3.84 \;\; 6.789 \;\; 1.658 \;\; 1.93 \;\; 38.7 \;\; 310]^T.$$

Fig. 6 shows the experimental stator-current slip curve (curve I) and the curves generated using the parameter vectors θ_0 (curve a: parameters obtained from classical tests) and θ_N (curve b: estimated parameters). Fig. 7 shows the experimental input-power slip curve (curve P) and the curve generated with the parameter vector θ_N (curve a).

TABLE I
PARAMETER VARIATION WITH PWM VOLTAGE SOURCE $l = 6$

f_s	**60Hz**	**30Hz**	**15Hz**
R_r	5.232	5.740	5.541
l_r	0.1273	0.1510	0.1667
l_s	0.1113	0.1451	0.1699
R_s	1.340	0.532	1.270
l_m	0.1023	0.1315	0.1502
R_{fe}	1145.5	304.6	116.0

TABLE II
PARAMETER VARIATION WITH PWM VOLTAGE SOURCE $l = 4$

f_s	**60Hz**	**30Hz**	**15Hz**
R_r	4.6436	5.306	5.1391
l_r	0.1128	0.1397	0.1529
l_s	0.1060	0.1265	0.1591
l_m	0.0928	0.1145	0.1362

Figs. 6 and 7 show that the curves generated with θ_N vector are close to the experimental ones. Also, they indicate that it is necessary to adjust the parameters obtained from the classical tests. For the data set collected from the experimental setup $J_{ip}(\theta) < 2.5 \times 10^{-3}$.

A. Parameter Variations

In the previous experimental tests, the induction machine has been supplied from a three-phase sinusoidal voltage source with low harmonic distortion. The parameters of the equivalent circuit change when the frequency of stator voltage is modified (i.e., slip variation, skin effect, deep bars, double cage). When the induction machine is supplied through a static power converter the presence of high-frequency harmonics also leads to changes in the parameters of the equivalent circuit.

To evaluate the influence of the harmonics on the equivalent circuit parameters, another experimental test has been conducted. In the test, a bipolar transistor inverter using the space-vector modulation technique supplies the three-phase stator voltage. The estimation algorithm is executed using two different parameter vectors: 1) the vector defined in (17) and 2) the vector defined in (18), where the R_s and R_{fe} are issued from the classical tests. Tables I and II show the results obtained for these two cases. It must be noted that the tables give the values of the machine's self inductances, as obtained from the estimation algorithm. Table I reveals that, using (17), the estimated R_s differs quite a lot from the measured one and varies from one frequency to another in a random way. However, when (18) is employed, the accuracy of the estimates clearly increases.

VI. CONCLUSIONS

The proposed nonlinear estimation algorithm allows one to determine the parameters of the induction machine. The algorithm is recursive and avoids the problem of dealing with ill-conditioned matrices that usually occurs in the nonlinear problems, using the inversion matrix lemma.

The estimation algorithm converges in a relatively fast way (less than 50 iterations). It yields good parameter estimates, without the necessity to constrain the parametric vector. The estimation algorithm is very simple to implement, since it requires the measurement of electrical quantities, only, and uses a recursive procedure. Also, the proposed procedure uses the data collected as recommended in the related IEEE Standard, and no special requirement is needed to conduct the experimental tests.

The particular form of the cost function $J(\theta)$ enabled the use of two data sources, without increasing the computational complexity. The choice of other, more suitable forms of $J(\theta)$, would be very interesting to investigate.

The present approach allows one to deal with a parameter vector whose length depends on the available *a priori* information about the equivalent model. This reasoning indicates that the use of parameter estimation techniques in determining the values of the equivalent circuit elements constitutes a promising tool in the modeling of electrical machines. The parameter set obtained with the proposed methodology may be used to start up the design of the ac drive system. On the other hand, if one decides to use parameter-estimation algorithms based on the dynamic models, this parameter set would be helpful in building a good initial parameter, which improves the convergence rate of the estimates.

APPENDIX

The analytical expressions of the derivatives of the input current $I(s)$ and the input power $P(s)$ with respect to each parameter are given below. The expressions given below are for a single-case induction machine.

A. Current Derivatives

$$\frac{\partial I(s)}{\partial R_r} = \frac{\partial I(s)}{\partial A}\frac{\partial A}{\partial R_r} + \frac{\partial I(s)}{\partial B}\frac{\partial B}{\partial R_r} + \frac{\partial I(s)}{\partial C}\frac{\partial C}{\partial R_r} + \frac{\partial I(s)}{\partial D}\frac{\partial D}{\partial R_r} \tag{28}$$

$$\frac{\partial I(s)}{\partial X_r} = \frac{\partial I(s)}{\partial A}\frac{\partial A}{\partial X_r} + \frac{\partial I(s)}{\partial B}\frac{\partial B}{\partial X_r} + \frac{\partial I(s)}{\partial C}\frac{\partial C}{\partial X_r} + \frac{\partial I(s)}{\partial D}\frac{\partial D}{\partial X_r} \tag{29}$$

$$\frac{\partial I(s)}{\partial X_s} = \frac{\partial I(s)}{\partial A}\frac{\partial A}{\partial X_s} + \frac{\partial I(s)}{\partial B}\frac{\partial B}{\partial X_s} + \frac{\partial I(s)}{\partial C}\frac{\partial C}{\partial X_s} + \frac{\partial I(s)}{\partial D}\frac{\partial D}{\partial X_s} \tag{30}$$

$$\frac{\partial I(s)}{\partial R_s}=\frac{\partial I(s)}{\partial A}\frac{\partial A}{\partial R_s}+\frac{\partial I(s)}{\partial B}\frac{\partial B}{\partial R_s}+\frac{\partial I(s)}{\partial C}\frac{\partial C}{\partial R_s}+\frac{\partial I(s)}{\partial D}\frac{\partial D}{\partial R_s} \quad (31)$$

$$\frac{\partial I(s)}{\partial X_m}=\frac{\partial I(s)}{\partial A}\frac{\partial A}{\partial X_m}+\frac{\partial I(s)}{\partial B}\frac{\partial B}{\partial X_m}+\frac{\partial I(s)}{\partial C}\frac{\partial C}{\partial X_m}+\frac{\partial I(s)}{\partial D}\frac{\partial D}{\partial X_m} \quad (32)$$

$$\frac{\partial I(s)}{\partial R_{fe}}=\frac{\partial I(s)}{\partial A}\frac{\partial A}{\partial R_{fe}}+\frac{\partial I(s)}{\partial B}\frac{\partial B}{\partial R_{fe}}+\frac{\partial I(s)}{\partial C}\frac{\partial C}{\partial R_{fe}}+\frac{\partial I(s)}{\partial D}\frac{\partial D}{\partial R_{fe}} \quad (33)$$

where

$$\frac{\partial I(s)}{\partial A}=-\frac{V\sqrt{C^2+D^2}A}{(A^2+B^2)^{3/2}} \quad \frac{\partial I(s)}{\partial B}=-\frac{V\sqrt{C^2+D^2}B}{(A^2+B^2)^{3/2}}$$
$$\frac{\partial I(s)}{\partial C}=\frac{VC}{\sqrt{C^2+D^2}\sqrt{A^2+B^2}}$$
$$\frac{\partial I(s)}{\partial D}=\frac{VD}{\sqrt{C^2+D^2}\sqrt{A^2+B^2}}.$$

B. Power Derivatives

$$\frac{\partial P(s)}{\partial R_r}=\frac{\partial P(s)}{\partial A}\frac{\partial A}{\partial R_r}+\frac{\partial P(s)}{\partial B}\frac{\partial B}{\partial R_r}+\frac{\partial P(s)}{\partial C}\frac{\partial C}{\partial R_r}+\frac{\partial P(s)}{\partial D}\frac{\partial D}{\partial R_r} \quad (34)$$

$$\frac{\partial P(s)}{\partial X_r}=\frac{\partial P(s)}{\partial A}\frac{\partial A}{\partial X_r}+\frac{\partial P(s)}{\partial B}\frac{\partial B}{\partial X_r}+\frac{\partial P(s)}{\partial C}\frac{\partial C}{\partial X_r}+\frac{\partial P(s)}{\partial D}\frac{\partial D}{\partial X_r} \quad (35)$$

$$\frac{\partial P(s)}{\partial X_s}=\frac{\partial P(s)}{\partial A}\frac{\partial A}{\partial X_s}+\frac{\partial P(s)}{\partial B}\frac{\partial B}{\partial X_s}+\frac{\partial P(s)}{\partial C}\frac{\partial C}{\partial X_s}+\frac{\partial P(s)}{\partial D}\frac{\partial D}{\partial X_s} \quad (36)$$

$$\frac{\partial P(s)}{\partial R_s}=\frac{\partial P(s)}{\partial A}\frac{\partial A}{\partial R_s}+\frac{\partial P(s)}{\partial B}\frac{\partial B}{\partial R_s}+\frac{\partial P(s)}{\partial C}\frac{\partial C}{\partial R_s}+\frac{\partial P(s)}{\partial D}\frac{\partial D}{\partial R_s} \quad (37)$$

$$\frac{\partial P(s)}{\partial X_m}=\frac{\partial P(s)}{\partial A}\frac{\partial A}{\partial X_m}+\frac{\partial P(s)}{\partial B}\frac{\partial B}{\partial X_m}+\frac{\partial P(s)}{\partial C}\frac{\partial C}{\partial X_m}+\frac{\partial P(s)}{\partial D}\frac{\partial D}{\partial X_m} \quad (38)$$

$$\frac{\partial P(s)}{\partial R_{fe}}=\frac{\partial P(s)}{\partial A}\frac{\partial A}{\partial R_{fe}}+\frac{\partial P(s)}{\partial B}\frac{\partial B}{\partial R_{fe}}+\frac{\partial P(s)}{\partial C}\frac{\partial C}{\partial R_{fe}}+\frac{\partial P(s)}{\partial D}\frac{\partial D}{\partial R_{fe}} \quad (39)$$

where

$$\frac{\partial P(s)}{\partial A}=\frac{3V^2C}{A^2+B^2}-\frac{6V^2(AC-BD)A}{(A^2+B^2)^2}$$
$$\frac{\partial P(s)}{\partial B}=-\frac{3V^2D}{A^2+B^2}-\frac{6V^2(AC-BD)B}{(A^2+B^2)^2}$$
$$\frac{\partial P(s)}{\partial C}=\frac{3V^2A}{A^2+B^2} \quad \frac{\partial P(s)}{\partial D}=-\frac{3V^2B}{A^2+B^2}$$
$$\frac{\partial A}{\partial R_r}=\frac{X_sR_{fe}}{X_ms}+\frac{R_s}{s}+\frac{R_{fe}}{s} \quad \frac{\partial B}{\partial R_r}=\frac{X_s}{s}-\frac{R_sR_{fe}}{X_ms}$$
$$\frac{\partial C}{\partial R_r}=\frac{1}{s} \quad \frac{\partial D}{\partial R_r}=\frac{R_{fe}}{X_ms}$$
$$\frac{\partial A}{\partial X_r}=-X_s+\frac{R_sR_{fe}}{X_m} \quad \frac{\partial B}{\partial X_r}=\frac{X_sR_{fe}}{X_m}+R_s+R_{fe}$$
$$\frac{\partial C}{\partial X_r}=\frac{R_{fe}}{X_m} \quad \frac{\partial D}{\partial X_r}=-1$$
$$\frac{\partial A}{\partial R_s}=\frac{R_r}{s}+R_{fe}\left(1+\frac{X_r}{X_m}\right) \quad \frac{\partial B}{\partial R_s}=-\frac{R_{fe}R_r}{X_ms}+X_r$$
$$\frac{\partial C}{\partial R_s}=0 \quad \frac{\partial D}{\partial R_s}=0$$
$$\frac{\partial A}{\partial X_s}=\frac{R_{fe}R_r}{X_ms}-X_r \quad \frac{\partial B}{\partial X_s}=\frac{R_r}{s}+R_{fe}\left(1+\frac{X_r}{X_m}\right)$$
$$\frac{\partial C}{\partial X_s}=0 \quad \frac{\partial D}{\partial X_s}=0$$
$$\frac{\partial A}{\partial X_m}=-\frac{X_sR_{fe}R_r}{X_m^2s}-\frac{R_sR_{fe}X_r}{X_m^2}$$
$$\frac{\partial B}{\partial X_m}=-\frac{X_sR_{fe}X_r}{X_m^2}+\frac{R_sR_{fe}R_r}{X_m^2s}$$
$$\frac{\partial C}{\partial X_m}=-\frac{R_{fe}X_r}{X_m^2} \quad \frac{\partial D}{\partial X_m}=-\frac{R_{fe}R_r}{X_m^2s}$$
$$\frac{\partial A}{\partial R_{fe}}=\frac{X_sR_r}{X_ms}+R_s\left(1+\frac{X_r}{X_m}\right)+\frac{R_r}{s}$$
$$\frac{\partial B}{\partial R_{fe}}=X_s\left(1+\frac{X_r}{X_m}\right)-\frac{R_sR_r}{X_ms}+X_r$$
$$\frac{\partial C}{\partial R_{fe}}=1+\frac{X_r}{X_m} \quad \frac{\partial D}{\partial R_{fe}}=\frac{R_r}{X_ms}.$$

References

[1] S. Ansuj, F. Shokooh, and R. Schinzinger, "Parameter estimation for induction machines based on sensitivity analysis," *IEEE Trans. Ind. Applicat.*, vol. 25, pp. 1035–1040, Nov./Dec. 1989.

[2] M. F. Al Turk, M. I. Mahmoud, and R. Perret, "An induction motor identification method for performance study and control strategy parameters determination," in *Conf. Rec. ICEM*, Pisa, Italy, 1988, pp. 271–276.

[3] M. Boussak and G. A. Capolino, "Modern control tools for identification of three phase induction motors," in *Conf. Rec. ICEM*, Pisa, Italy, 1988, pp. 215–220.

[4] J. Hickiewicz, K. Macek-Kaminska, and P. Wach, "Algorithmic methods of induction machines parameters estimation from measured slip-curves," *Arch. Elektrotech.*, vol. 1, no. 72, pp. 239–249, 1989.

[5] J. Hickiewicz, K. Macek-Kaminska, and P. Wach, "Simulation investigations and parameter estimation of induction machine's model considering saturation of leakage inductances," in *Conf. Rec. ICEM*, Pisa, Italy, 1988, pp. 238–244.

[6] M. Velez-Reyes, K. Minami, and G. C. Verghese, "Recursive speed and parameter estimation for induction machines," in *Conf. Rec. IAS Annu. Meeting*, 1989, pp. 607–611.

[7] J. Stephan, M. Bodson, and J. Chiasson, "Real-time estimation of the parameters and fluxes of induction motors," *IEEE Trans. Ind. Applicat.*, vol. 30, pp. 746–759, May/June 1994.

[8] J. A. DeKock, F. S. Van der Merwe, and H. J. Vermeulen, "Induction motor parameter estimation through an output error technique," *IEEE Trans. Energy Conversion*, vol. 9, pp. 69–76, Mar. 1994.
[9] IEEE Standards Board, "Electric machinery," in *IEEE Standard Test Procedure for Polyphase Induction Motors and Generators*. Piscataway, NJ: IEEE Press, 1995.
[10] J. Chatelain, *Machines Electriques, Vol. 1*. Paris, France: Dunod, 1983.
[11] N. R. Draper and H. Smith, *Applied Regression Analysis*. New York: Wiley, 1981.
[12] L. Ljung, *System Identification: Theory for the User*. Englewood Cliffs, NJ: Prentice-Hall, 1987.
[13] D. Graupe, *Identification of Systems*. New York: Van Nostrand-Reinhold, 1972.

Antonio Marcus Nogueira Lima (S'77–M'89) was born in Recife, Pernambuco, Brazil, in 1958. He received the Bachelor's and Master's degrees in electrical engineering from the Federal University of Paraíba, Campina Grande, Paraíba, Brazil, in 1982 and 1985, respectively, and the doctoral degree from the Institut National Polytechnique de Toulouse, Toulouse, France, in 1989.

He was with the Escola Técnica Redentorista, Campina Grande, Paraíba, Brazil, from 1977 to 1982 and was a Project Engineer with Sul-América Philips, Recife, Pernambuco, Brazil, from 1982 to 1983. Since September 1983, he has been a Faculty Member in the Electrical Engineering Department, Federal University of Paraíba. His research interests are in the fields of electrical machines and drives, electronic instrumentation, control systems, and system identification.

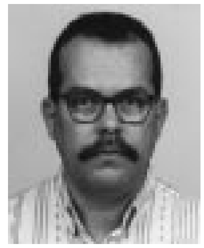

Cursino Brandão Jacobina (S'78–M'78) was born in Correntes, Pernambuco, Brazil, in 1955. He received the Bachelor's degree in electrical engineering from the Federal University of Paraíba, Campina Grande, Paraíba, Brazil, in 1978 and the Diplôme d'Etudes Approfondies (DEA) and the doctoral degrees from the Institut National Polytechnique de Toulouse, Toulouse, France, in 1980 and 1983, respectively.

Since 1978, he has been a Faculty Member in the Electrical Engineering Department, Federal University of Paraíba. His research interests include electrical drives, power electronics, control systems, and system identification.

Eurico Bezerra de Souza Filho was born in Recife, Pernambuco, Brazil, in 1956. He received the Bachelor's and Master's degrees in electrical engineering from the Federal University of Pernambuco, Recife, Pernambuco, Brazil, in 1979 and 1982, respectively, and the doctoral degree from the Federal University of Paraíba, Campina Grande, Paraíba, Brazil, in 1993.

Since 1980, he has been a Faculty Member in the Electrical Engineering Department, Federal University of Pernambuco. His research interests include electrical drives and power electronics.